

University of Groningen

Light-harvesting Complexes (LHCs) Cluster Spontaneously in Membrane Environment Leading to Shortening of Their Excited State Lifetimes

Natali, Alberto; Gruber, J. Michael; Dietzel, Lars; Stuart, Marc C. A.; van Grondelle, Rienk; Croce, Roberta

Published in:
The Journal of Biological Chemistry

DOI:
[10.1074/jbc.M116.730101](https://doi.org/10.1074/jbc.M116.730101)

IMPORTANT NOTE: You are advised to consult the publisher's version (publisher's PDF) if you wish to cite from it. Please check the document version below.

Document Version
Publisher's PDF, also known as Version of record

Publication date:
2016

[Link to publication in University of Groningen/UMCG research database](#)

Citation for published version (APA):

Natali, A., Gruber, J. M., Dietzel, L., Stuart, M. C. A., van Grondelle, R., & Croce, R. (2016). Light-harvesting Complexes (LHCs) Cluster Spontaneously in Membrane Environment Leading to Shortening of Their Excited State Lifetimes. *The Journal of Biological Chemistry*, 291(32), 16730-16739. <https://doi.org/10.1074/jbc.M116.730101>

Copyright

Other than for strictly personal use, it is not permitted to download or to forward/distribute the text or part of it without the consent of the author(s) and/or copyright holder(s), unless the work is under an open content license (like Creative Commons).

The publication may also be distributed here under the terms of Article 25fa of the Dutch Copyright Act, indicated by the "Taverne" license. More information can be found on the University of Groningen website: <https://www.rug.nl/library/open-access/self-archiving-pure/taverne-amendment>.

Take-down policy

If you believe that this document breaches copyright please contact us providing details, and we will remove access to the work immediately and investigate your claim.

Downloaded from the University of Groningen/UMCG research database (Pure): <http://www.rug.nl/research/portal>. For technical reasons the number of authors shown on this cover page is limited to 10 maximum.

Light-harvesting Complexes (LHCs) Cluster Spontaneously in Membrane Environment Leading to Shortening of Their Excited State Lifetimes*

Received for publication, March 30, 2016, and in revised form, May 24, 2016 Published, JBC Papers in Press, June 1, 2016, DOI 10.1074/jbc.M116.730101

Alberto Natali^{‡1}, J. Michael Gruber^{‡1}, Lars Dietzel[§], Marc C. A. Stuart[¶], Rienk van Grondelle[‡], and Roberta Croce^{‡‡}

From the [‡]Department of Physics and Astronomy, Faculty of Sciences, VU University Amsterdam, 1081 HV Amsterdam, The Netherlands, [§]Institute of Molecular Biosciences, Goethe-University Frankfurt/M, 60438 Frankfurt, Germany, and

[¶]Electron Microscopy, Groningen Biomolecular Sciences and Biotechnology Institute, University of Groningen, 9747 AG Groningen, The Netherlands

The light reactions of photosynthesis, which include light-harvesting and charge separation, take place in the amphiphilic environment of the thylakoid membrane. The light-harvesting complex II (LHCII) is the main responsible for light absorption in plants and green algae and is involved in photoprotective mechanisms that regulate the amount of excited states in the membrane. The dual function of LHCII has been extensively studied in detergent micelles, but recent results have indicated that the properties of this complex differ in a lipid environment. In this work we checked these suggestions by studying LHCII in liposomes. By combining bulk and single molecule measurements, we monitored the fluorescence characteristics of liposomes containing single complexes up to densely packed proteoliposomes. We show that the natural lipid environment *per se* does not alter the properties of LHCII, which for single complexes remain very similar to that in detergent. However, we show that LHCII has the strong tendency to cluster in the membrane and that protein interactions and the extent of crowding modulate the lifetimes of the excited state in the membrane. Finally, the presence of LHCII monomers at low concentrations of complexes per liposome is discussed.

Photosynthetic organisms evolved the capacity to harvest the energy of solar radiation and store it into chemical compounds. In vascular plants and green algae, sunlight is absorbed by a series of membrane proteins called light-harvesting complexes (LHC).³ The most abundant of these pigment-protein complexes is LHCII. The LHCs have a dual function; in low light conditions they absorb solar energy and efficiently transfer the excitation energy to the reaction center, and in high light they

additionally play a role in photoprotection by dissipating the energy absorbed in excess as heat (1, 2). This last process called non-photochemical quenching (NPQ) leads to a decrease of the excited state lifetime of chlorophyll *a* (Chl *a*), limiting the possibility of Chl triplet formation and thus the production of singlet oxygen (3). The fast, on the timescale of seconds, and fully reversible part of NPQ is called qE. This mechanism is triggered by the acidification of the lumenal space of the thylakoids, which activates PsbS (4) and LhcSR (5), the proteins responsible for NPQ in plants and green algae, respectively, and the violaxanthin de-epoxidase, which converts violaxanthin into zeaxanthin (for reviews, see Refs. 6 and 7). Although the precise molecular mechanism of quenching has not been fully elucidated yet, a prominent idea discussed in literature is that NPQ is regulated via conformational changes of LHCII. Those changes could be correlated to, or even caused by, LHCII aggregation (8, 9). It was observed that low pH and zeaxanthin, both occurring in high light, enhance LHCII aggregation (10). Aggregation of LHCII *in vitro* is accompanied by a decrease of the Chl *a* fluorescence yield, indicating an increased rate of energy dissipation (9, 11). The generation of new quenching sites is assumed to occur either via pigment-pigment interactions at the protein-protein interface or within the protein as a result of conformational changes (6, 12). Although the effect of aggregation on fluorescence quenching *in vitro* is clearly demonstrated, its role in NPQ *in vivo* is still under debate (13, 14).

The study of NPQ *in vivo* is complicated by the presence of many parallel processes that make it difficult to extract its molecular details. A large part of the studies on NPQ has then been performed *in vitro* on isolated complexes in detergent micelles. However, these preparations represent an over-simplified system in a non-native environment. To overcome these problems, several approaches have been put forward: (i) reducing the number of components involved in NPQ in the thylakoid membrane by using mutants lacking photosystems I and II core complexes or blocking the chloroplast translation that leads to membranes enriched in LHCII (15, 16) and (ii) studying isolated LHCII in detergent-free environment using nanodisks (17), styrene maleic acid (18), amphipoles (19), or liposomes (20–22). These methods have revealed that the lifetime of LHCII in the membrane differs substantially from its lifetime in detergent micelles, suggesting that in the natural environment the antennas assume a different and more quenched conformation.

* This work was supported by the European Research Council (ERC) Consolidator Grant 281341 (ASAP) and by the Dutch organization for scientific research NWO via a Vici grant (to R. C.). The work was also supported by ERC Advanced Investigation Grant 267333 (to R. v. G.) and by the Humboldt Foundation in the course of a Feodor-Lynen fellowship (to L. D.). The authors declare that they have no conflicts of interest with the contents of this article.

¹ Both authors contributed equally to this work.

² To whom correspondence should be addressed. Tel.: 31-20-59-86310; Fax: 31-20-5987999; E-mail: r.croce@vu.nl.

³ The abbreviations used are: LHCII, light harvesting complex II; NPQ, non-photochemical quenching; Chl *a*, chlorophyll *a*; Chl *b*, chlorophyll *b*; Tricine, N-[2-hydroxy-1,1-bis(hydroxymethyl)ethyl]glycine; Qy, light absorption due to electronic transition along the y-axis of the chlorophyll molecule.

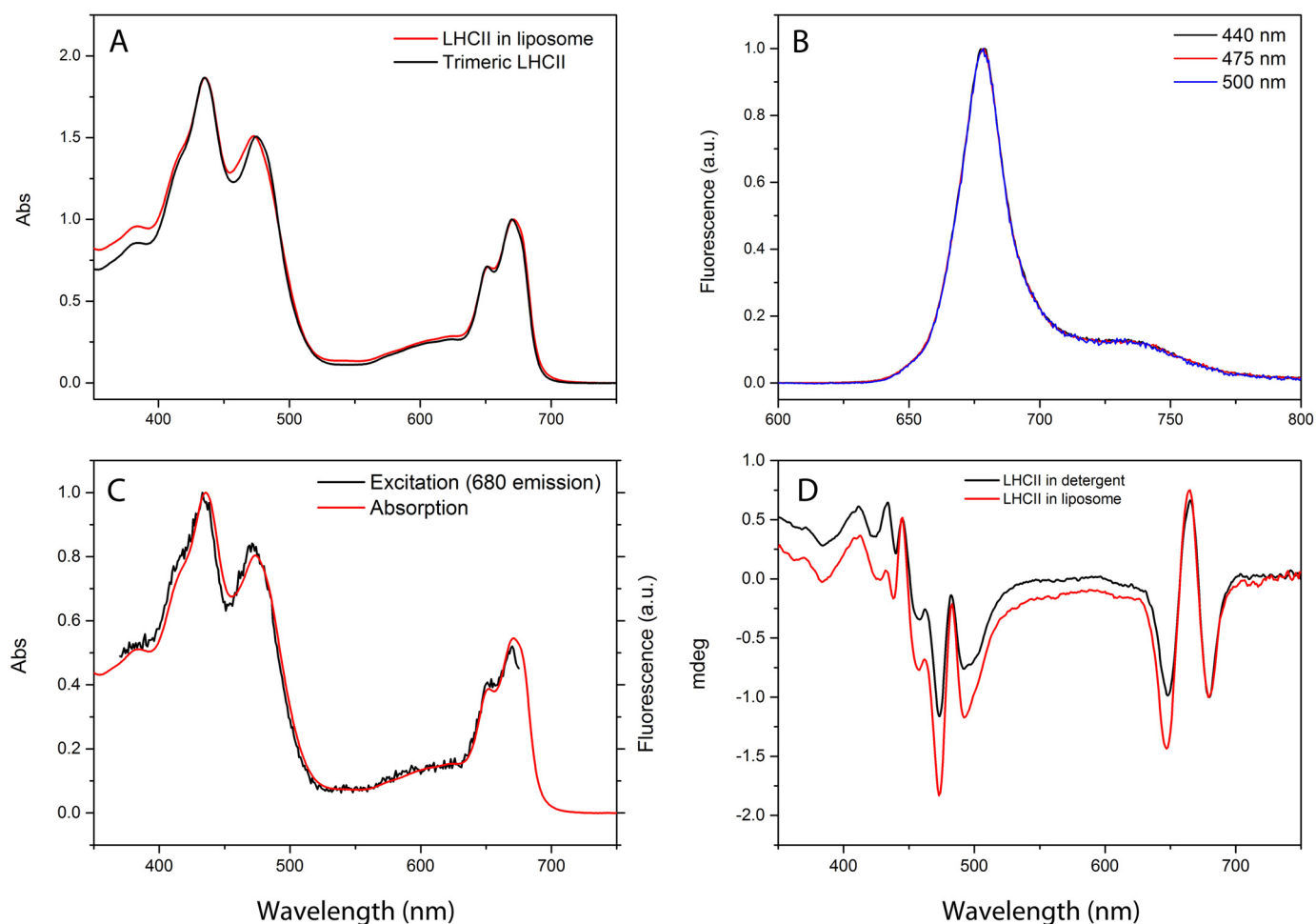


FIGURE 1. Spectroscopic analysis of proteoliposomes. *A*, absorption spectra of isolated LHCII solubilized in detergent and incorporated into lipid vesicles. The spectra are normalized to the maximum in the Qy region. *B*, fluorescence emission spectra normalized to the maximum. *a.u.*, arbitrary units. *C*, fluorescence excitation spectra recorded at very low concentrations (when 1-Transmission is equal to the absorption) compared with the absorption spectrum normalized to 1. *D*, CD spectra normalized to the negative signal at 679 nm.

The advantage provided by liposomes in the study of light-harvesting is their flexibility; they permit the analysis of the characteristic of the antennas by varying lipid composition (21) and protein/lipid ratio (20). They make it possible to change in the composition of the membrane in a controlled way and to study the effect of the presence of different pigments or proteins on the properties of the complexes (23, 24). These characteristics make proteoliposomes an attractive system to investigate in detail the mechanism of NPQ in a lipid bilayer environment. Liposomes containing zeaxanthin and PsbS, which are two essential factors in NPQ, in addition to LHCII were described (24, 25), opening way to study the molecular mechanism of NPQ *in vitro*. However, to be able to disentangle the effect of lateral aggregation, conformational switches, and protein-lipid interactions, all of which have been suggested to play a role in NPQ, it is essential to know how the lipid environment influences the properties of the complex and to have full control of their organization in the proteoliposome.

In this work we investigated in detail the relation between protein crowding and the fluorescence decay, which is the reporter for the quenched state of the complexes, by generating a series of proteoliposomes with different lipid/Chl ratios. Using a combination of ensemble and single molecule spectroscopy

measurements we show that the different properties observed in LHCII in the membrane, as compared with detergent micelles, are not due to a different conformation of single complexes caused by the lipid environment but due to the clustering of LHCII. The latter most likely leads to conformational changes due to protein-protein interactions. The similarity with the results in cells suggests that this is what happens *in vivo*.

Results

Incorporation of *Chlamydomonas reinhardtii* LHCII into Liposome Vesicles—To mimic the thylakoid membrane of *C. reinhardtii*, we generated liposome vesicles composed of an identical mix of lipids: monogalactosyl diacylglycerol (41.2%), digalactosyl diacylglycerol (26.7%), sulfoquinovosyl diacylglycerols (15.6%), and the phospholipids (11.5%) and phosphatidylcholine (5%) (26). Antenna complexes (LHCII) isolated from the membranes (Fig. 1) or reconstituted *in vitro* with pigments (Fig. 2) were incorporated into liposome vesicles by the removal of detergent via dialysis. The initial preparation consists of a lipid/protein molar ratio of ~230:1. The resulting proteoliposomes show absorption maxima at 672 nm and 436 nm with shoulders at 651 nm and 473 nm. The absorption spectrum is

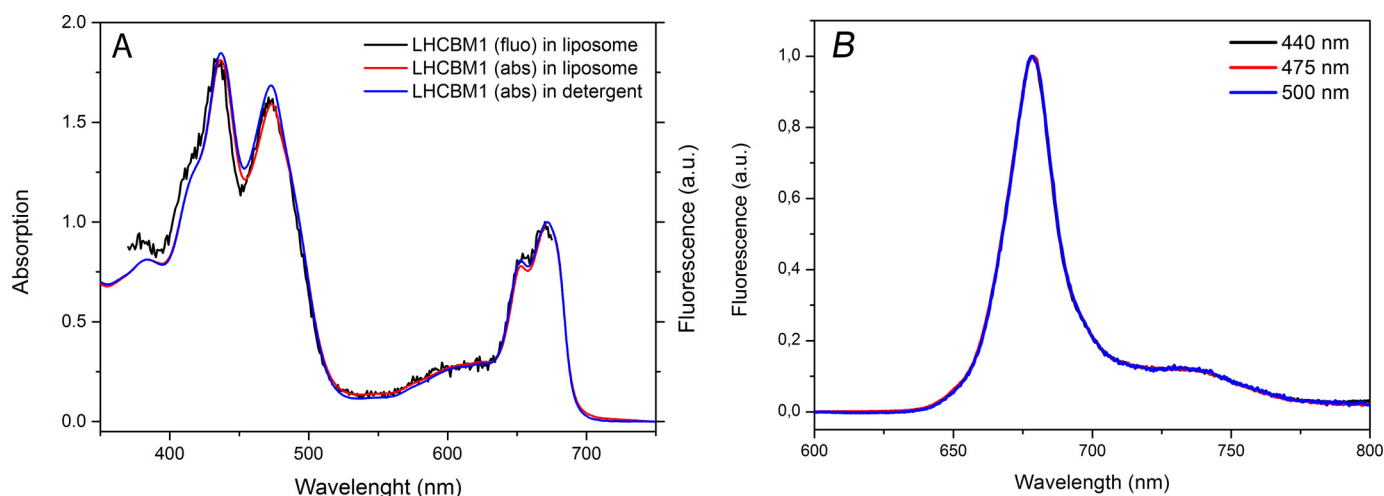


FIGURE 2. **Spectroscopic characterization of reconstituted monomeric LHCBM1 incorporated into liposomes.** A, absorption (in detergent and in liposome) and fluorescence excitation spectra of the recombinant protein. The spectra are normalized to the maximum in the Qy region. B, fluorescence emission spectra normalized to the maximum. *a.u.*, arbitrary units.

shown in Fig. 1A where it is compared with that of detergent-isolated LHCII trimers. In general, no large differences were observed between the spectra, indicating that the incorporation into liposomes does not lead to loss of pigments. These features are in agreement with previously published works on LHCII incorporated into liposomes (21, 25, 27).

The fluorescence emission spectrum of the LHCII-containing liposomes at room temperature (Fig. 1B) consists of a single peak with a maximum at 680 nm upon excitation of Chl *a* (440 nm), Chl *b* (475 nm), and carotenoids (500 nm). This indicates that the excitation energy is efficiently transferred from Chl *b* and carotenoids to Chl *a*, which confirms the correct folding of the complexes. The high efficiency of excitation energy transfer is further supported by the fluorescence excitation spectrum (Fig. 1C).

The CD spectrum depicted in Fig. 1D confirms that LHCII in liposomes and detergent have the same pigment organization. The spectrum clearly shows the typical $-+ -$ signal in the Qy absorption region and the negative CD feature in the blue region associated with Chl-Chl and Chl-carotenoid interactions (28).

Aggregation of LHCII in Liposomes—It is known that *in vitro* aggregation of LHCII is accompanied by a decrease of the fluorescence quantum yield (9, 23). This phenomenon, which is induced *in vitro* by the removal of detergent, may also occur during or after the incorporation of the complexes into liposomes, complicating the interpretation of the results. We note that the topology of aggregation might be different in solution and in the plane of a lipid bilayer, where mainly lateral aggregates are expected. However, the topology of insertion of the complexes in the liposomes is undetermined, and we cannot exclude the presence of interactions between complexes with opposite orientation. The formation of lateral aggregates in liposomes (at a lipid/protein molar ratio of $\sim 230:1$) is confirmed by the fluorescence emission spectra at 77 K (Fig. 3A), which shows a peak at 696 nm typical of aggregated antennas (29). Aggregation, quantified by the relative intensity of the 696 nm band, decreased by reducing the amount of LHCII per liposome (Fig. 3B). By recording the fluorescence decay kinetics of

LHCII at different levels of aggregation, we could also confirm the tight relation between lateral aggregation and fluorescence quenching. Fig. 3B clearly illustrates that the peak at 696 nm increased with the increase of the amount of chlorophyll per liposome. At the same time, the fluorescence lifetime decreased down to a minimum of 0.97 ns (Table 1). On the other hand, the lifetime of the sample in liposomes with a high lipid/protein molar ratio of $\sim 7000:1$ (0.1 μg of Chl *a*) had a similar value compared with isolated monomeric LHCII in detergent (Table 1) (30, 31). A further decrease in the amount of protein per liposome (0.05 μg of Chl *a* equal to a lipid/protein molar ratio of $\sim 14,000:1$) induced the appearance of free Chls in the sample. This is indicated by the presence of a shoulder at 650 nm in the fluorescence emission spectrum upon selective Chl *b* excitation (Fig. 3B) and by a long lifetime component above 4 ns in the time-resolved data, typical of free chlorophylls (Table 1).

Electron Microscopy (EM) and Single Molecule Spectroscopy—The structure and size of liposomes were investigated by EM. In Fig. 4 EM images of proteoliposomes containing LHCII (Fig. 4A) and recombinant LHCBM1 (Fig. 4B) showed a homogeneous morphology and size distribution. The average diameter of the proteoliposomes was ~ 50 nm, and no indication of multi-lamellar structures was observed.

To acquire more quantitative information on the composition of proteoliposomes and hence on the level of protein aggregation, we performed single molecule confocal fluorescence experiments and analyzed the fluorescence intensity, the fluorescence spectrum, and the fluorescence lifetime of single immobilized proteoliposomes. The information about the absolute fluorescence intensity together with the average fluorescence lifetime allowed us to approximate the absorption cross-section σ of the fluorescence particle within the confocal excitation (see “Experimental Procedures”). This effectively provides the size of the cluster via the number of absorbing pigments. By dividing the absorption cross-section of a single fluorescent particle (*i.e.* a single proteoliposome) by the absorption cross-section of a LHCII trimer at 633 nm ($\sigma_{\text{LHCII}} = 1.4 \times 10^{-15} \text{ cm}^2$) we can estimate the number of incorporated

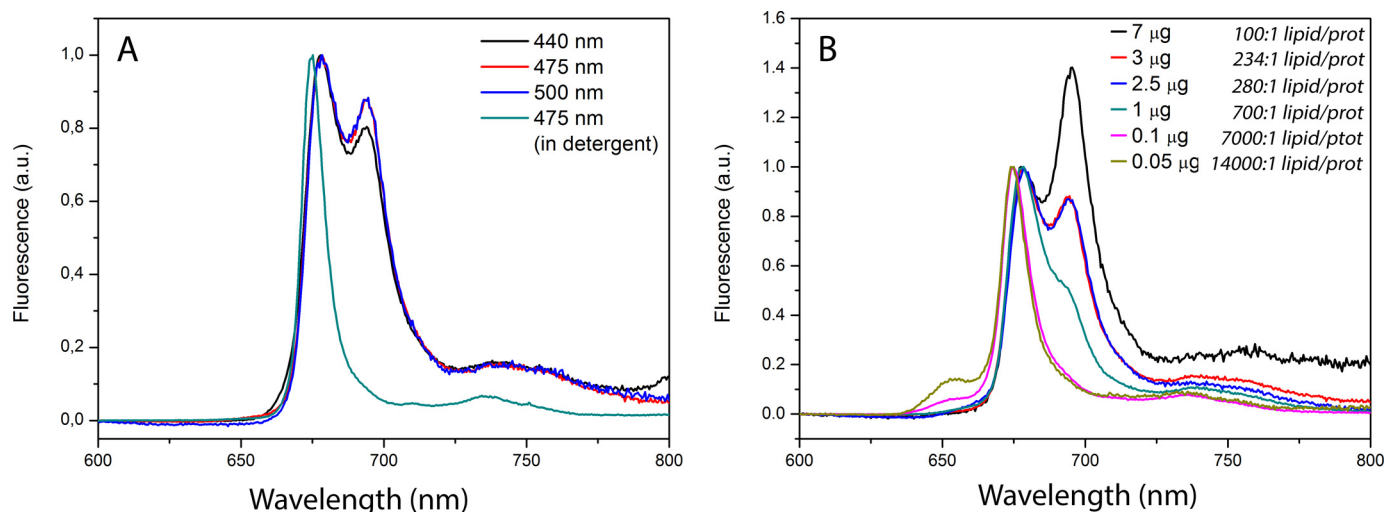


FIGURE 3. **Fluorescence emission spectra of LHCII liposomes at 77 K.** *A*, comparison with LHCII in detergent (234:1 lipid/protein molar ratio) after excitation of Chl *a* (440 nm), Chl *b* (475 nm), and carotenoids (500 nm). The spectra are normalized to the maximum. *B*, fluorescence emission spectra of LHCII in liposomes at different concentrations after excitation of Chl *b* (475 nm). The lipid/protein molar ratio are shown in the legend with the amount of Chl *a* used for each preparation. The spectra are normalized at 680 nm. *a.u.*, arbitrary units.

TABLE 1

Excited-state lifetimes of proteoliposomes with different amounts of LHCII

The amplitudes (A_i) of the different lifetimes (τ_i) to fluorescence decay and the average fluorescence lifetimes (τ_{ave}) are given.

LHCII (μg Chl <i>a</i>)	τ_{ave}	A_1	τ_1	A_2	τ_2	A_3	τ_3
	<i>ns</i>	%	<i>ns</i>	%	<i>ns</i>	%	<i>ns</i>
7	0.97	35	0.41	57	1.14	8	2.22
3	1.84	23	0.56	56	1.89	21	3.12
2.5	1.36	35	0.53	56	1.59	8	3.26
1	2.12	26	0.72	62	2.34	11	4.21
0.1	3.34	11	1.06	70	3.21	19	5.20
0.05	3.49	9	0.92	75	3.37	16	5.52

LHCII. Fig. 5A shows the resulting distribution of proteoliposomes with a low and high protein concentration and a control experiment on LHCII trimers in detergent. To make sure that we were measuring LHCII in liposomes and not random aggregates in solution, we performed a control experiment without lipids at detergent concentrations below the CMC, which leads to protein aggregation in solution. This experiment yielded different results than LHC complexes within liposomes (data not shown). In particular, large protein aggregates were formed in solution as indicated by a significantly increased fluorescence intensity compared with proteoliposomes at an identical protein-liposome ratio. In agreement with this, the density of detected fluorescent particles per imaging area decreased for aggregates in solution. These results indicate that it is possible to discriminate between lateral aggregation of LHCII in liposomes and random aggregates in solution and that all the experiments reported below were conducted on LHCII in liposomes. The high concentrated sample contains dozens of LHCII trimers with a peak at ~ 30 trimers. The *dotted black line* in Fig. 5A indicates the hypothetical situation in which the complete surface of a liposome with a 50-nm diameter is fully covered with LHCII. This implies that LHCII complexes constitute a significant fraction of the surface area of a single proteoliposome and explains the aggregation features observed in bulk measurements. The fluorescence intensity of those large aggregates shows a gradual decrease over time most likely caused by

bleaching and light-induced formation of energy traps that can influence a large number of connected complexes. Proteoliposomes with the lowest protein concentration of $\sim 7000:1$ lipid/protein molar ratio instead show clear reversible intensity steps, often referred to as “blinking,” characteristic for individual light-harvesting complexes. Fig. 5B illustrates some typical examples of such fluorescence time traces for the highest (*black line*) and lowest protein concentration (*light- and dark blue line*). It should be noted that at very low concentrations the number of LHC complexes per liposome varies from one to three, but in all cases the LHCII blink individually. The corresponding fluorescence lifetimes are plotted in Fig. 5C. The decrease in lifetime for a larger number of incorporated LHC complexes matches the trend seen in ensemble measurements. Fig. 5D shows a distribution of the measured fluorescence intensity and fluorescence lifetime for proteoliposomes at the indicated protein density. The slope of such a distribution depends among other parameters on the absorption cross-section and, therefore, also indicates the size distribution of the measured particles. A decreasing slope corresponds to a larger absorption cross-section as indicated by the *red arrow* in Fig. 5D. The lifetimes of proteoliposomes with $7 \mu\text{g}$ of Chl *a* (lipid/protein molar ratio of 100:1) are shorter (~ 450 ps) than measured in the ensemble due to the much higher excitation intensity, which can generate light-induced traps. The lifetime of single complexes instead matches very well with the dominating 3-ns lifetime component found in bulk. The long lifetime shown for the *light blue* example in Fig. 5B demonstrates that individual complexes are either poorly connected or more likely floating in the bilayer completely isolated from each other. Blinking events, partial quenching, and bleaching of individual complexes instead results in an additional shorter lifetime component, but the long lifetime component of other isolated complexes is not affected.

A surprising outcome was the low absolute fluorescence intensity of single complexes (at $0.1 \mu\text{g}$ of Chl *a*) that is only $\sim 35\%$ that of the expected value for LHCII trimers. It actually

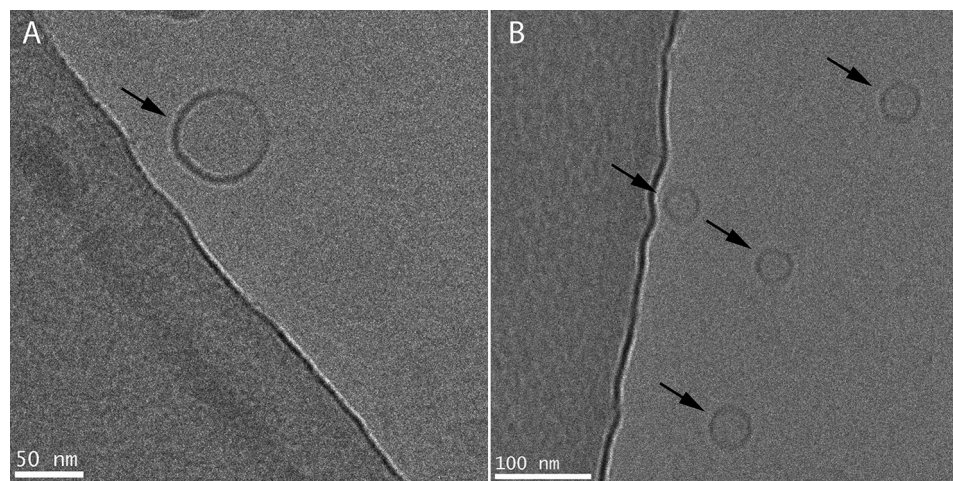


FIGURE 4. **Electron micrographs of proteoliposomes showing the size and the shape of the vesicles (black arrows).** A, proteoliposomes containing LHCII. B, proteoliposomes containing reconstituted LHCBM1.

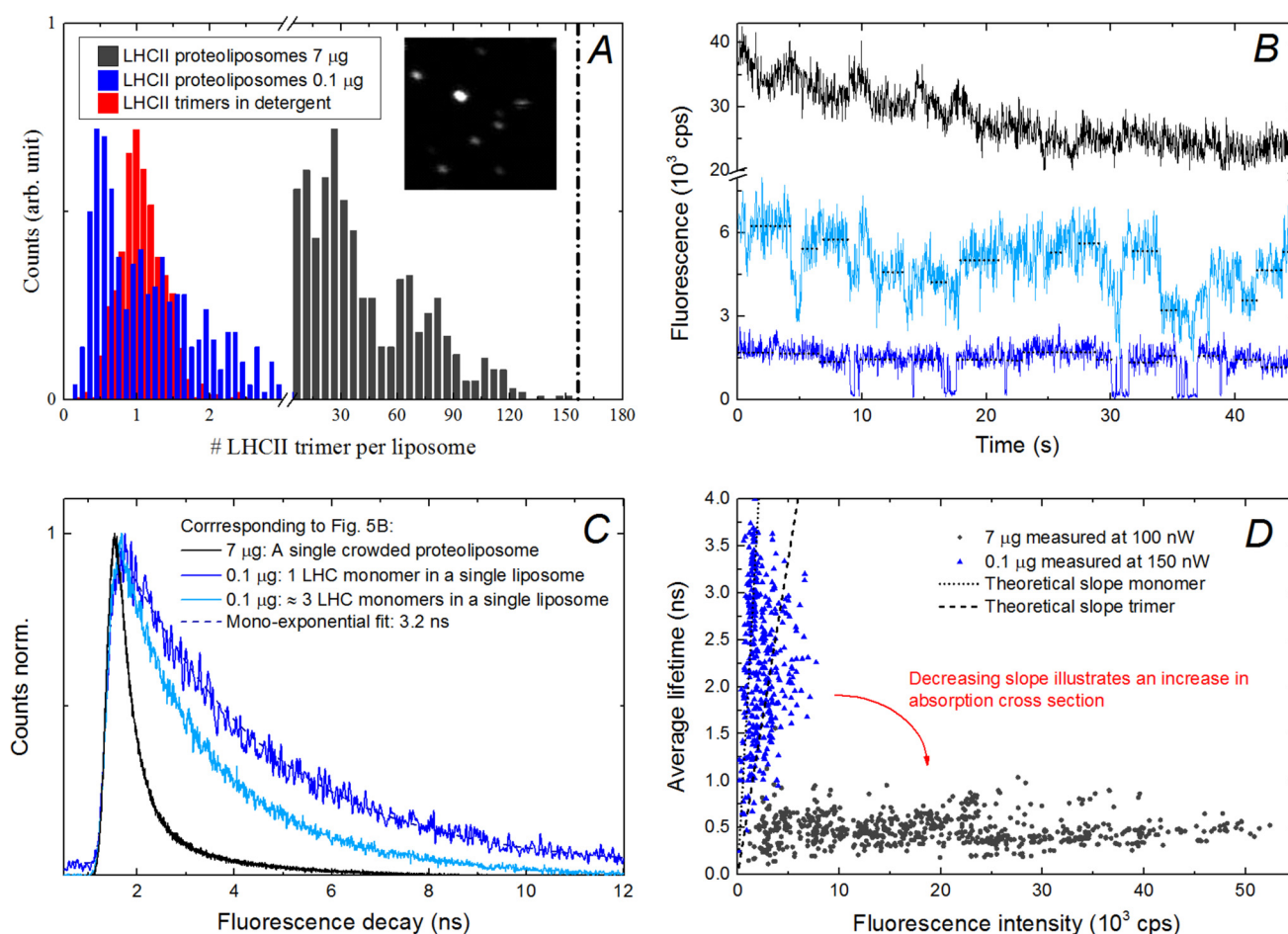


FIGURE 5. **Single molecule fluorescence measurements.** A, histogram of the estimated number of trimeric LHCII complexes associated with one bright spot found in confocal fluorescence images of surface-bound proteoliposomes. The red histogram represents a control experiment on trimeric LHCII complexes in detergent. The first peak at \sim 30 complexes of proteoliposomes with a high concentration of protein can be assigned to single proteoliposomes; larger values might also represent multiple liposomes within the confocal excitation spot. The blue histogram clearly shows the presence of monomeric LHCII complexes. The black dotted line indicates the hypothetical surface area of a sphere (diameter of 50 nm) purely made out of LHCII complexes. The inset illustrates a typical fluorescence image. arb., arbitrary units. B, exemplary fluorescence intensity traces of three LHCII proteoliposomes corresponding to the indicated protein concentration. The light and dark blue traces correspond to two different proteoliposomes from the same sample concentration of 0.1 μ g of Chl *a*. The black dotted lines indicate exemplary intensity levels used for the lifetime analysis in D. C, the corresponding fluorescence decays of the fluorescence traces in Fig. 5B. The blue dotted line indicates a mono-exponential fit. D, the average lifetime corresponding to individual intensity levels for liposomes with the highest and lowest protein density. The slope in such a graph is an indication of the absorption cross and, therefore, clearly demonstrates the difference in the number of incorporated complexes. A smaller slope corresponds to a larger absorption cross-section as indicated by the red arrow. The dotted lines show the calculated slopes for an LHC monomer and LHCII trimer for comparison.

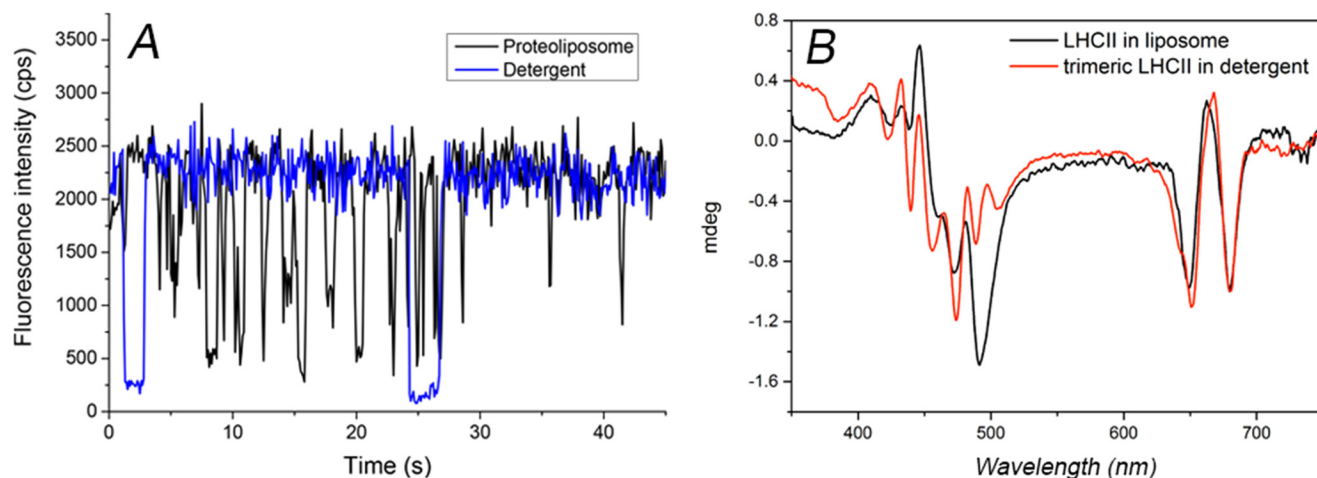


FIGURE 6. **Monomers versus trimers.** A, exemplary fluorescence intensity traces of monomeric LHCBM1 complexes in detergent (black line) and incorporated into a liposome (blue line). We want to note that the apparent difference in blinking rates is random and cannot be interpreted from the behavior of a single complex. B, circular dichroism analysis of LHCII in liposome and in detergent. Normalized to the negative peak at 679 nm.

better matches the fluorescence intensity of monomeric LHC complexes than that of the trimer. The absorption cross-section distribution for that sample in Fig. 5A also clearly shows a peak at less than half a trimeric complex. Interestingly, most of the proteoliposomes with 0.1 μg of Chl *a* ($\sim 7000:1$ lipid/protein molar ratio) show a fluorescence intensity equivalent to $\sim 1:3$ monomeric complexes. To further clarify this monomerization effect, we measured proteoliposomes that were loaded directly with monomeric LHCBM1 ($\sim 7000:1$ lipid/protein molar ratio), and here we indeed found a matching fluorescence intensity between isolated monomeric complexes in detergent and single complexes in liposomes (see Fig. 6A). Finally, we confirmed the monomeric state of incorporated LHC complexes using LHCII from plants, the CD spectrum of which differs for monomers and trimers (28); LHCII trimers of tobacco inserted into liposomes show a CD spectrum typical for the monomeric state (Fig. 6B) (28).

A remaining question concerns the presence of free pigments in proteoliposomes. To that end, we recorded multiple fluorescence spectra (1-s integration time) of single proteoliposomes, which allows us to follow the spectral evolution over 30 s. The majority of measured proteoliposomes (LHCII; 7000:1 lipid/protein molar ratio) indeed exhibits a small blue shoulder below 680 nm as illustrated in Fig. 7. The amplitude of that shoulder varies between different particles but always decreases exponentially in time, and only the main emission peak at 681 nm remains. Control experiments on liposomes that contained only free Chl (not shown) displayed the same exponential bleaching feature and had a fluorescence peak emission of 678 nm, matching the blue shoulder peak found in proteoliposomes.

Discussion

One of the main challenges in studying the mechanisms of photoprotection and the related regulatory components is the tradeoff between *in vivo* measurements, which are hard to interpret on a molecular scale, and *in vitro* experiments that usually fail to mimic the native and possibly essential thylakoid membrane environment. Proteoliposomes, where light-har-

vesting complexes are embedded in a lipid bilayer that contains the lipids of the thylakoid membrane, are becoming a popular system to study antenna complexes *in vitro* (20, 21, 24, 25, 27, 32, 33). With the aim to mimic the thylakoid membrane, highly concentrated proteoliposomes with a lipid/protein molar ratio between ~ 30 –600:1 are used. Here we show that the aggregation feature in the fluorescence emission spectra at 77 K disappears only at a lipid/protein molar ratio of $\sim 7000:1$ (equal to 0.1 μg of Chl *a* in our liposome preparation), whereas lower lipid/protein ratios result in different levels of aggregations, which are characterized by different fluorescence lifetimes. It is thus important to closely monitor the lipid/protein ratio in the liposomes to avoid complications due to differences in the aggregation states of the samples.

By coupling bulk and single molecule measurements, we show that it is possible to control the amount of incorporated complexes from dozens of proteins down to a single complex per liposome, demonstrating that LHCII in a lipid environment, but in the absence of aggregation/clustering, is in an unquenched state. In fact, the fluorescence decay of most single complexes in the light harvesting state (“on-state” in blinking) can be fitted with a single lifetime component of ~ 3 ns, equivalent to that of detergent-isolated complexes. Even proteoliposomes that contain up to three or four monomeric complexes show this long lifetime component, as the complexes are apparently not connected and emit individually. This clearly demonstrates that the lipid environment and the interaction of the complexes with lipids do not *per se* lead to a quenched conformation. Our results instead suggest that protein-protein interactions and crowding are the main reasons for the shorter lifetime observed for LHCII in the membrane.

A somewhat surprising result is that trimeric LHCII disassemble to monomers upon incorporation into liposomes. This effect is unexpected as LHCII trimers are very stable even in detergent environment (34), and it has been shown that trimerization is favored by the presence of lipids (35). One possibility is that the surface curvature of liposomes, which corresponds to an angular change of $\sim 10^\circ$ within 5 nm, facilitates

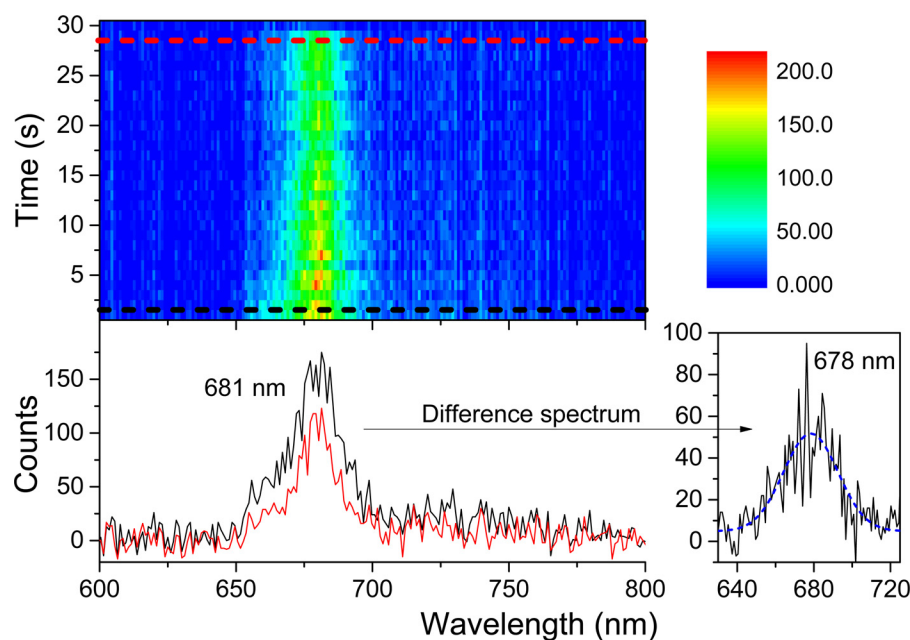


FIGURE 7. **Fluorescence spectra of single molecules.** *Top*, contour plot of the spectral evolution of a single complex over a time period of 30 s. The integration time of one spectrum was 1 s. *Bottom*, extracted fluorescence spectra as indicated in the top contour plot by the red and black line. The difference spectrum to the right shows the emission peak of free chlorophyll.

monomerization. Indeed, it has been shown that the curvature represents a stress that induces modification in some membrane proteins (36). Interestingly, such a degree of curvature is similar to that of the grana margin of the thylakoid membrane (37). These regions are particularly important for the regulation of association of LHCII with the two photosystems (38) and for the disassembling/repairing of photosystem II (39). It is thus tempting to speculate that the membrane curvature helps in the dissociation of multiprotein complexes. Indeed monomerization of LHCII has been observed in high light (40). Contrary to detergent micelles that effectively constrain and, therefore, facilitate the trimeric structure, reversible binding rates of monomeric subunits in a freely floating trimer might very well lead to the stochastically determined disassociation of the trimeric structure.

Finally, the fact that the blinking feature of single LHC complexes, well described for detergent-isolated complexes and assumed to be involved in NPQ (41), is confirmed in a lipid bilayer environment supports its functional relevance in native systems. Even proteoliposomes with a high protein density (black line in Fig. 5) show reversible intensity fluctuations that can be caused either by a few isolated complexes or more likely by switching events that affect a whole domain of connected complexes.

In conclusion, based on the controlled variation in lipid/protein ratio and the concomitant determination of the LHCII aggregation together with its spectroscopic properties, we conclude that LHCII has the tendency to cluster in the membrane, and we suggest that this clustering induces a conformational change of LHCII that controls the concentration of the excited states. We observe clustering already in the presence of a molar lipid to protein ratio of $\sim 700:1$, a condition in which LHCII is much more diluted than in the thylakoid membrane. This suggests that *in vivo* in its native membrane LHCII are normally clustered, which explains their shorter lifetime compared with isolated complexes.

Experimental Procedures

Strain, Growth Conditions, and Thylakoid Preparations—*C. reinhardtii* cells (strain JVD-1B[pGG1]) were grown in tris acetate phosphate liquid medium (42) at 25 °C under mild agitation (170 rpm) and 50 μmol of photons $\text{PAR m}^{-2} \text{s}^{-1}$. Thylakoid membrane isolation was performed as described in Fischer *et al.* (43) with modifications reported in Drop *et al.* (44). Briefly, the cells were disrupted by sonication (60 watts power in 10 cycles of 10 s on/30 s off) and centrifuged at $17,000 \times g$ at 4 °C for 20 min. Purification of thylakoid membranes was performed using a discontinuous gradient in a SW41 swinging bucket rotor (24,000 rpm, 1 h, 4 °C).

Isolation of Light Harvesting Complexes—The isolation of LHCII was achieved following the protocol described in Drop *et al.* (30). In brief, unstacked thylakoids were solubilized in α -dodecylmaltoside detergent. The sample was fractionated by sucrose gradient density centrifugation. The green bands (LHCII) were harvested with a syringe.

In Vitro Reconstitution of Recombinant LHCII—The reconstitution of LHCBM1 was done as described in (45). In short, the apoprotein overexpressed in *Escherichia coli* and purified from inclusion bodies was mixed with pigments extracted from *C. reinhardtii*. The reconstituted protein was then purified by nickel affinity chromatography, taking advantage of a His tag on the C terminus of the protein and by sucrose density gradient centrifugation.

Liposome Preparation and Incorporation of LHCII—For liposome preparation we used a modified protocol from Gundermann and Büchel (46). The thylakoid lipids monogalactosyl diacylglycerol, digalactosyl diacylglycerol, sulfoquinovosyl diacylglycerols, phosphatidylglycerol, and phosphatidylcholine were purchased from Larodan Fine Chemicals (Malmö, Sweden), already dissolved in chloroform. Lipids were mixed in the

following relative molar ratios: 41.2% monogalactosyl diacylglycerol, 26.7% digalactosyl diacylglycerol, 15.6% sulfoquinovosyl diacylglycerols, 11.5% phosphatidylglycerol, and 5% phosphatidylcholine (26). The chloroform was slowly removed under N₂ vapor to form a thin film of lipids on the inner wall of the vial. 85 μ g of lipids were rehydrated using 29 μ l of 10% octyl glucoside solution and mixed overnight at 4 °C. Then 221 μ l of 20 mM Tricine solution (pH 7.5) and 250 μ l of dialysis buffer 4 \times (80 mM Tricine (pH 7.5), 20 mM MgCl₂, and 0.04% sodium azide) were added to the lipid solution. Extrusion was performed 10 \times through a 0.2- μ m filter using the Extruder set (Avanti Polar Lipids, Inc.). The sample was diluted in a total volume of 125 μ l dialysis buffer 1 \times and mixed with 125 μ l of the lipid suspension. The final solution was then subjected to 3 cycles of vortexing (5 min) and incubation on ice (5 min). Finally, to remove the detergent and incorporate the protein into liposomes, the sample was dialyzed (14 kDa Viskin dialysis membrane) for 2 days in a dialysis buffer in ice. During the second day Biobeads-SM2 (Bio-Rad) were added to the dialysis buffer to remove the remaining detergent. The sample was then centrifuged for 30 min at 25,000 \times g at 4 °C. The supernatant was collected and transferred in another tube.

Absorption, Circular Dichroism (CD), and Steady State Fluorescence Measurements—Room temperature absorption spectra were recorded with a Cary 4000 spectro-photometer (Varian). The CD spectra were measured using a Chirascan CD spectrophotometer (Applied-Photophysics). Fluorescence emission spectra were recorded using a Fluorolog 3.22 spectrofluorimeter (Jobin Yvon-Spex). The excitation wavelengths were 440, 475, and 500 nm, and emission was detected in the 600–800-nm range. Excitation and emission bandwidths were set to 3 nm. All fluorescence spectra were measured at an absorbance of 0.05 cm⁻¹ at the maximum of the Qy absorption band. Room temperature measurements were performed in 0.5 M sucrose, 20 mM Hepes (pH 7.5), and 0.06% α -dodecylmaltoside buffer. For 77 K measurements a liquid nitrogen cooled device was used (cold finger).

Time-correlated Single Photon Counting—Time-resolved fluorescence measurements were performed using a FluoTime 200 fluorometer (PicoQuant). The samples were diluted to an absorbance of 0.05 cm⁻¹ at the Qy maximum and stirred in a cuvette with a path length of 1 cm. Excitation was provided by a 470-nm laser diode with a repetition rate of 10 MHz and a power of 5 microwatts. Fluorescence emission at 680 nm was collected under an angle of 90° with respect to the excitation. All measurements were performed at 283 K, and the maximum number of counts in the peak channel was 20,000. Kinetics were analyzed after deconvolution from the instrument response function and measured with a pinacyanol iodide dye dissolved in methanol in which the lifetime is \sim 6 ps (47). Full width at half maximum of the instrument response function was \sim 80 ps. Global analysis was made using the TRFA Data Processor Advanced software.

Electron Microscopy—A 3- μ l sample was applied on a holey carbon-coated grid (Quantifoil 3.5/1), blotted, and vitrified using a Vitrobot (FEI). Frozen hydrated samples were observed in an FEI Technai T20 electron microscope operating at 200 keV, equipped with a Gatan model 626 cryo-stage. Images were recorded on a slow-scan CCD camera under low dose conditions.

Single Molecule Spectroscopy—Proteoliposomes were immobilized on poly-L-lysine-coated microscope cover glasses, and the measuring solution (1 \times dialysis buffer) within the closed sample chamber contained an oxygen scavenging mix (2.5 mM protocatechuic acid, 25 nM protocatechuate-3,4-dioxygenase) to avoid photo-bleaching via singlet oxygen formation. The concentration of proteoliposomes was empirically adjusted to achieve a surface density of <10 particles per fluorescence image (5 \times 5 μ m). The rupture of vesicles upon nonspecific surface binding cannot be excluded, but surface coating with poly-L-lysine has been reported to prevent disruption of lipid vesicles on the bare glass interface and is a standard technique for cell and protein adhesion (48, 49). Single particles were excited at 633 nm with a repetition rate of 76 MHz (Coherent Mira 900F coupled to a Coherent MIRA OPO), and fluorescence spectra, intensities, and lifetimes were measured at room temperature on a home-built confocal fluorescence setup as described in detail earlier (50). In short, the fluorescence intensity was detected with avalanche photodiodes (Micro Photon Devices, PDM series, instrument response function of 38 ps or SPCM-AQR-16, PerkinElmer Optoelectronics, instrument response function of 304 ps), and fluorescence decay histograms were obtained via time-correlated single photon counting (PicoHarp 300, PicoQuant) and fitted with a deconvolution algorithm in FluoFit (PicoQuant). Fluorescence intensity traces were binned into 30-ms time steps, and the fluorescence decay traces were binned into 4-ps intervals. Fluorescence spectra with an integration time of 1 s were obtained by dispersing the collected fluorescence via a grating (HR830/800 nm, Optometrics LLC) onto a CCD camera (Spec10:100BR, Roper Scientific). The relative absorption cross-section of identified particles can be calculated as,

$$\sigma = \frac{k_{\text{abs}}}{I_e/E_{\text{photon}}} \quad (\text{Eq. 1})$$

with

$$k_{\text{abs}} = \frac{1}{\eta t_{\text{acq}}} \sum_i \frac{A_i \tau_i}{t_{\text{bin}} \varphi_i} = \frac{\sum A_i}{\eta t_{\text{acq}} t_{\text{bin}} k_f} \quad (\text{Eq. 2})$$

where k_{abs} is the photon absorption rate, I_e is the excitation intensity, E_{photon} is the energy of a fluorescence photon (680 nm), η is the overall detection efficiency of the confocal setup, t_{acq} is the acquisition time, t_{bin} is the binning time of the fluorescence decay histogram, and A_i and τ_i are the amplitudes and lifetimes of the fitted multi-exponential fluorescence decay.

Author Contributions—R. C. conceived the study. A. N. and J. M. G. conducted most of the experiments and analyzed the results. L. D. set up the liposome system. M. C. A. S. performed the electron microscopy. R. v. G. provided access to the single molecule spectroscopy setup. A. N., J. M. G., and R. C. wrote the paper. All authors approved the final version of the manuscript.

References

1. Croce, R., and van Amerongen, H. (2014) Natural strategies for photosynthetic light harvesting. *Nat. Chem. Biol.* **10**, 492–501

2. Rochaix, J.-D. (2014) Regulation and dynamics of the light-harvesting system. *Annu. Rev. Plant Biol.* **65**, 287–309
3. Roach, T., and Krieger-Liszka, A. (2014) Regulation of photosynthetic electron transport and photoinhibition. *Curr. Protein Pept. Sci.* **15**, 351–362
4. Li, X. P., Björkman, O., Shih, C., Grossman, A. R., Rosenquist, M., Jansson, S., and Niyogi, K. K. (2000) A pigment-binding protein essential for regulation of photosynthetic light harvesting. *Nature* **403**, 391–395
5. Peers, G., Truong, T. B., Ostendorf, E., Busch, A., Elrad, D., Grossman, A. R., Hippler, M., and Niyogi, K. K. (2009) An ancient light-harvesting protein is critical for the regulation of algal photosynthesis. *Nature* **462**, 518–521
6. Ruban, A. V., Johnson, M. P., and Duffy, C. D. (2012) The photoprotective molecular switch in the photosystem II antenna. *Biochim. Biophys. Acta* **1817**, 167–181
7. Niyogi, K. K., and Truong, T. B. (2013) Evolution of flexible non-photochemical quenching mechanisms that regulate light harvesting in oxygenic photosynthesis. *Curr. Opin. Plant Biol.* **16**, 307–314
8. Jahns, P., Depka, B., and Trebst, A. (2000) Xanthophyll cycle mutants from *Chlamydomonas reinhardtii* indicate a role for zeaxanthin in the D1 protein turnover. *Plant Physiol. Biochem.* **38**, 371–376
9. Horton, P., Ruban, A. V., Rees, D., Pascal, A. A., Noctor, G., and Young, A. J. (1991) Control of the light-harvesting function of chloroplast membranes by aggregation of the LHCII chlorophyll-protein complex. *FEBS Lett.* **292**, 1–4
10. Ruban, A. V., Phillip, D., Young, A. J., and Horton, P. (1997) Carotenoid-dependent oligomerization of the major chlorophyll *a/b* light harvesting complex of photosystem II of plants. *Biochemistry* **36**, 7855–7859
11. Wentworth, M., Ruban, A. V., and Horton, P. (2000) Chlorophyll fluorescence quenching in isolated light harvesting complexes induced by zeaxanthin. *FEBS Lett.* **471**, 71–74
12. Bassi, R., and Caffarri, S. (2000) Lhc proteins and the regulation of photosynthetic light harvesting function by xanthophylls. *Photosynth. Res.* **64**, 243–256
13. Horton, P., Wentworth, M., and Ruban, A. (2005) Control of the light harvesting function of chloroplast membranes: the LHCII-aggregation model for non-photochemical quenching. *FEBS Lett.* **579**, 4201–4206
14. Jahns, P., and Holzwarth, A. R. (2012) The role of the xanthophyll cycle and of lutein in photoprotection of photosystem II. *Biochim. Biophys. Acta* **1817**, 182–193
15. Tian, L., Dinc, E., and Croce, R. (2015) LHCII populations in different quenching states are present in the thylakoid membranes in a ratio that depends on the light conditions. *J. Phys. Chem. Lett.* **6**, 2339–2344
16. Belgio, E., Johnson, M. P., Jurić, S., and Ruban, A. V. (2012) Higher plant photosystem II light-harvesting antenna, not the reaction center, determines the excited-state lifetime—both the maximum and the nonphotochemically quenched. *Biophys. J.* **102**, 2761–2771
17. Borch, J., and Hamann, T. (2009) The nanodisc: a novel tool for membrane protein studies. *Biol. Chem.* **390**, 805–814
18. Bell, A. J., Frankel, L. K., and Bricker, T. M. (2015) High Yield non-detergent isolation of photosystem I-light-harvesting chlorophyll II membranes from spinach thylakoids: implications for the organization of the PS I antennae in higher plants. *J. Biol. Chem.* **290**, 18429–18437
19. Liguori, N., Roy, L. M., Opacic, M., Durand, G., and Croce, R. (2013) Regulation of light harvesting in the green alga *Chlamydomonas reinhardtii*: the C terminus of LHCSR is the knob of a dimmer switch. *J. Am. Chem. Soc.* **135**, 18339–18342
20. Zhou, F., Liu, S., Hu, Z., Kuang, T., Paulsen, H., and Yang, C. (2009) Effect of monogalactosyldiacylglycerol on the interaction between photosystem II core complex and its antenna complexes in liposomes of thylakoid lipids. *Photosynth. Res.* **99**, 185–193
21. Yang, C., Boggasch, S., Haase, W., and Paulsen, H. (2006) Thermal stability of trimeric light-harvesting chlorophyll *a/b* complex (LHCIIb) in liposomes of thylakoid lipids. *Biochim. Biophys. Acta* **1757**, 1642–1648
22. Wardak, A., Brodowski, R., Krupa, Z., and Gruszecki, W. I. (2000) Effect of light-harvesting complex II on ion transport across model lipid membranes. *J. Photochem. Photobiol. B.* **56**, 12–18
23. Kirchhoff, H., Hinz, H.-J., and Rösger, J. (2003) Aggregation and fluorescence quenching of chlorophyll *a* of the light-harvesting complex II from spinach *in vitro*. *Biochim. Biophys. Acta* **1606**, 105–116
24. Wilk, L., Grunwald, M., Liao, P.-N., Walla, P. J., and Kühlbrandt, W. (2013) Direct interaction of the major light-harvesting complex II and PsbS in nonphotochemical quenching. *Proc. Natl. Acad. Sci. U.S.A.* **110**, 5452–5456
25. Liu, C., Gao, Z., Liu, K., Sun, R., Cui, C., Holzwarth, A. R., and Yang, C. (2016) Simultaneous refolding of denatured PsbS and reconstitution with LHCII into liposomes of thylakoid lipids. *Photosynth. Res.* **127**, 109–116
26. Vieler, A., Wilhelm, C., Goss, R., Süß, R., and Schiller, J. (2007) The lipid composition of the unicellular green alga *Chlamydomonas reinhardtii* and the diatom *Cyclotella meneghiniana* investigated by MALDI-TOF MS and TLC. *Chem. Phys. Lipids* **150**, 143–155
27. Moya, I., Silvestri, M., Vallon, O., Cinque, G., and Bassi, R. (2001) Time-resolved fluorescence analysis of the photosystem II antenna proteins in detergent micelles and liposomes. *Biochemistry* **40**, 12552–12561
28. Georgakopoulou, S., van der Zwan, G., Bassi, R., van Grondelle, R., van Amerongen, H., and Croce, R. (2007) Understanding the changes in the circular dichroism of light harvesting complex II upon varying its pigment composition and organization. *Biochemistry* **46**, 4745–4754
29. Ruban, A. V., Calkoen, F., Kwa, S. L. S., Van Grondelle, R., Horton, P., and Dekker, J. P. (1997) Characterisation of LHC II in the aggregated state by linear and circular dichroism spectroscopy. *Biochim. Biophys. Acta* **1321**, 61–70
30. Drop, B., Webber-Birungi, M., Yadav, S. K., Filipowicz-Szymanska, A., Fusetti, F., Boekema, E. J., and Croce, R. (2014) Light-harvesting complex II (LHCII) and its supramolecular organization in *Chlamydomonas reinhardtii*. *Biochim. Biophys. Acta* **1837**, 63–72
31. Natali, A., and Croce, R. (2015) Characterization of the major light-harvesting complexes (LHCBM) of the green alga *Chlamydomonas reinhardtii*. *PLoS ONE* **10**, e0119211
32. Iwaszko, E., Wardak, A., Krupa, Z., and Gruszecki, W. I. (2004) Ion transport across model lipid membranes containing light-harvesting complex II: an effect of light. *J. Photochem. Photobiol. B.* **74**, 13–21
33. Haferkamp, S., and Kirchhoff, H. (2008) Significance of molecular crowding in grana membranes of higher plants for light harvesting by photosystem II. *Photosynth. Res.* **95**, 129–134
34. Croce, R., Weiss, S., and Bassi, R. (1999) Carotenoid-binding sites of the major light-harvesting complex II of higher plants. *J. Biol. Chem.* **274**, 29613–29623
35. Hobe, S., Prytulla, S., Kühlbrandt, W., and Paulsen, H. (1994) Trimerization and crystallization of reconstituted light-harvesting chlorophyll *a/b* complex. *EMBO J.* **13**, 3423–3429
36. van den Brink-van der Laan, E., Killian, J. A., and de Kruijff, B. (2004) Nonbilayer lipids affect peripheral and integral membrane proteins via changes in the lateral pressure profile. *Biochim. Biophys. Acta* **1666**, 275–288
37. Armbruster, U., Labs, M., Pribil, M., Viola, S., Xu, W., Scharfenberg, M., Hertle, A. P., Rojahn, U., Jensen, P. E., Rappaport, F., Joliet, P., Dörmann, P., Wanner, G., and Leister, D. (2013) *Arabidopsis* curvature thylakoid 1 proteins modify thylakoid architecture by inducing membrane curvature. *Plant Cell* **25**, 2661–2678
38. Suorsa, M., Rantala, M., Mamedov, F., Lespinasse, M., Trotta, A., Grieco, M., Vuorio, E., Tikkanen, M., Järvi, S., and Aro, E.-M. (2015) Light acclimation involves dynamic re-organization of the pigment-protein megacomplexes in non-appressed thylakoid domains. *Plant J.* **84**, 360–373
39. Puthiyaveetil, S., Tsabari, O., Lowry, T., Lenhert, S., Lewis, R. R., Reich, Z., and Kirchhoff, H. (2014) Compartmentalization of the protein repair machinery in photosynthetic membranes. *Proc. Natl. Acad. Sci. U.S.A.* **111**, 15839–15844
40. Bielczynski, L. W., Schansker, G., and Croce, R. (2016) Effect of light acclimation on the organization of photosystem II super- and sub-complexes in *Arabidopsis thaliana*. *Front. Plant Sci.* **7**, 105
41. Krüger, T. P., Iliaia, C., Johnson, M. P., Ruban, A. V., and van Grondelle, R. (2014) Disentangling the low-energy states of the major light-harvesting complex of plants and their role in photoprotection. *Biochim. Biophys. Acta* **1837**, 1027–1038

42. Gorman, D. S., and Levine, R. P. (1965) Cytochrome f and plastocyanin: their sequence in the photosynthetic electron transport chain of *Chlamydomonas reinhardtii*. *Proc. Natl. Acad. Sci. U.S.A.* **54**, 1665–1669
43. Fischer, N., Sétif, P., and Rochaix, J. D. (1997) Targeted mutations in the *psaC* gene of *Chlamydomonas reinhardtii*: preferential reduction of FB at low temperature is not accompanied by altered electron flow from photosystem I to ferredoxin. *Biochemistry* **36**, 93–102
44. Drop, B., Webber-Birungi, M., Fusetti, F., Kouřil, R., Redding, K. E., Boekema, E. J., and Croce, R. (2011) Photosystem I of *Chlamydomonas reinhardtii* contains nine light-harvesting complexes (Lhca) located on one side of the core. *J. Biol. Chem.* **286**, 44878–44887
45. Natali, A., Roy, L. M., and Croce, R. (2014) *In Vitro* Reconstitution of light-harvesting complexes of plants and green algae. *J. Vis. Exp.* **92**, e51852
46. Gundermann, K., and Büchel, C. (2012) Factors determining the fluorescence yield of fucoxanthin-chlorophyll complexes (FCP) involved in non-photochemical quenching in diatoms. *Biochim. Biophys. Acta* **1817**, 1044–1052
47. van Oort, B., Amunts, A., Borst, J. W., van Hoek, A., Nelson, N., van Amerongen, H., and Croce, R. (2008) Picosecond fluorescence of intact and dissolved PSI-LHCI crystals. *Biophys. J.* **95**, 5851–5861
48. Rossetti, F. F., Reviakine, I., Csúcs, G., Assi, F., Vörös, J., and Textor, M. (2004) Interaction of poly(L-lysine)- γ -poly(ethylene glycol) with supported phospholipid bilayers. *Biophys. J.* **87**, 1711–1721
49. Akashi, K., Miyata, H., Itoh, H., and Kinoshita, K. (1998) Formation of giant liposomes promoted by divalent cations: critical role of electrostatic repulsion. *Biophys. J.* **74**, 2973–2982
50. Gruber, J. M., Chmeliov, J., Krüger, T. P., Valkunas, L., and van Grondelle, R. (2015) Singlet-triplet annihilation in single LHCI complexes. *Phys. Chem. Chem. Phys.* **17**, 19844–19853

Light-harvesting Complexes (LHCs) Cluster Spontaneously in Membrane Environment Leading to Shortening of Their Excited State Lifetimes
Alberto Natali, J. Michael Gruber, Lars Dietzel, Marc C. A. Stuart, Rienk van Grondelle
and Roberta Croce

J. Biol. Chem. 2016, 291:16730-16739.

doi: 10.1074/jbc.M116.730101 originally published online June 1, 2016

Access the most updated version of this article at doi: [10.1074/jbc.M116.730101](https://doi.org/10.1074/jbc.M116.730101)

Alerts:

- [When this article is cited](#)
- [When a correction for this article is posted](#)

[Click here](#) to choose from all of JBC's e-mail alerts

This article cites 50 references, 7 of which can be accessed free at
<http://www.jbc.org/content/291/32/16730.full.html#ref-list-1>